nature astronomy

Article

https://doi.org/10.1038/s41550-023-01998-8

A long-duration gamma-ray burst of dynamical origin from the nucleus of an ancient galaxy

Received: 9 February 2023

Accepted: 5 May 2023

Published online: 22 June 2023



Andrew J. Levan 1,2 , Daniele B. Malesani 1,3,4,5 , Benjamin P. Gompertz 6 , Anya E. Nugent, Matt Nicholl, Samantha R. Oates 6 , Daniel A. Perley, Jillian Rastinejad 0 , Brian D. Metzger, Steve Schulze 11 , Elizabeth R. Stanway 11 , Anne Inkenhaag, Tayyaba Zafar, Kornpob Bhirombhakdi 11 , J. Feliciano Agüí Fernández 11 , Ashley A. Chrimes, Kornpob Bhirombhakdi 11 , Antonio de Ugarte Postigo 11 , Wen-fai Fong, Andrew S. Fruchter 11 , Giacomo Fragione 11 , Johan P. U. Fynbo 11 , Nicola Gaspari 11 , Kasper E. Heintz, Jens Hjorth, Pall Jakobsson 11 , Peter G. Jonker 11 , Gavin P. Lamb 11 , Ilya Mandel 11 , Soheb Mandhai 11 , Maria E. Ravasio, Jesper Sollerman 11 , Will R. Tanvir 11

The majority of long-duration (>2 s) gamma-ray bursts (GRBs) arise from the collapse of massive stars, with a small proportion created from the merger of compact objects. Most of these systems form via standard stellar evolution pathways. However, a fraction of GRBs may result from dynamical interactions in dense environments. These channels could also contribute substantially to the samples of compact object mergers detected as gravitational wave sources. Here we report the case of GRB 191019A, a long GRB (a duration of $T_{90} = 64.4 \pm 4.5$ s), which we pinpoint close (\$100 pc projected) to the nucleus of an ancient (>1 Gyr old) host galaxy at z = 0.248. The lack of evidence for star formation and deep limits on any supernova emission disfavour a massive star origin. The most likely route for progenitor formation is via dynamical interactions in the dense nucleus of the host. The progenitor, in this case, could be a compact object merger. These may form in dense nuclear clusters or originate in a gaseous disc around the supermassive black hole. Identifying, to the best of our knowledge, a first example of a dynamically produced GRB demonstrates the role that such bursts may have in probing dense environments and constraining dynamical fractions in gravitational wave populations.

Routes to stellar death

The evolution of most stars in the Universe is dominated by their stellar or binary evolution. However, for a small fraction in dense environments additional many-body interactions enable new channels to the formation of exotic stellar systems. These systems include the

formation of compact object binaries whose subsequent merger creates high frequency gravitational wave sources as well as, in some cases, gamma-ray bursts $^{1-3}$. In addition to many-body interactions, capture processes in gas rich discs around supermassive black holes can also create such binaries 4 .

A full list of affiliations appears at the end of the paper. —e-mail: a.levan@astro.ru.nl

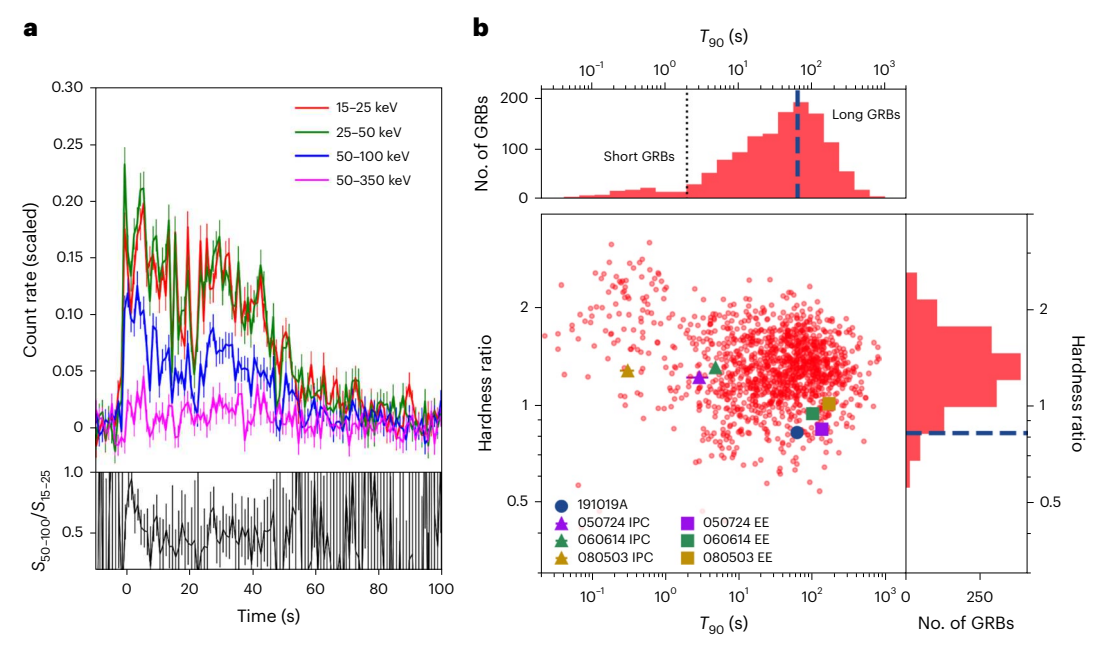


Fig. 1 | **The gamma-ray properties of GRB 191019A. a**, The gamma-ray light curve of GRB 191019A as observed by the Swift BAT. The burst consists of a single emission episode, with additional intrinsic variability. The burst begins with a short spike, but it is neither especially hard, nor separated from the bulk of the emission. The lower panel shows the hardness ratio between the count rates (*S*) in the 50–100 keV and 15–25 keV bands, which demonstrates some degree of spectral softening, with the initial peak being the hardest emission episode.

b, The location of GRB 191019A on the hardness–duration plane. The background red points represent bursts from the Swift BAT catalog 95 , while GRB 191019A is indicated with the dark blue circle. Also marked are the locations of bursts identified as short + extended emission (EE) based on the duration of their initial pulse complex (IPC) and extended emission separately. The properties of GRB 191019A are comparable with the properties of the extended emission component in other bursts.

If the merging compact objects include a neutron star or white dwarf, then the merger can also yield luminous electromagnetic radiation. The identification of a short gamma-ray burst (GRB) and a kilonova with the gravitational-wave-detected binary neutron-star merger GW170817 secured the connection of mergers with short GRBs. While long GRBs are generally thought to arise from extreme core-collapse supernovae $^{11-13}$, recent evidence suggests that a subset also form via the mergers of compact objects $^{14-16}$.

The supernova-less GRB 191019A

GRB 191019A was detected by the Neil Gehrels Swift Observatory (hereafter Swift) at 15:12:33 UT on 19 October 2019¹⁷. The burst is characterized by a fast rise and slower decay with additional variability superimposed (Fig. 1). The duration is measured to be $T_{90} = 64.4 \pm 4.5$ s (ref. 18), which is hence classified as a long GRB. The burst is relatively soft with a power-law photon index of $\Gamma = 2.25 \pm 0.05$. Its fluence is $S = (1.00 \pm 0.03) \times 10^{-7}$ erg cm⁻² (15–150 keV)¹⁸.

Spacecraft constraints prevented a prompt slew by Swift, and observations with the X-ray telescope (XRT) and the ultraviolet and optical telescope (UVOT) began 52 minutes after the burst. These revealed an X-ray and a UV afterglow¹⁹. We obtained optical observations of the field with the Nordic Optical Telescope (NOT) beginning 4.52 hours after the burst²⁰. Comparison with later epochs reveals a faint afterglow positionally consistent with the nucleus of the host galaxy visible in each of the g, r, i and z bands (Fig. 2). Spectroscopy obtained with the NOT on 19 October 2019, and confirmed with the Gemini South telescope on 1 December 2019, found a redshift of z = 0.248 based on several absorption lines, including Ca H, Ca K and the hydrogen Balmer series (Fig. 3). The standard star-forming emission lines are notably absent from these spectra, which suggests an old galaxy.

Following these observations, we obtained deep imaging in the *g*, *r* and *z* bands from the NOT and the Gemini South telescope from 2 to 73 days after the burst and optical imaging with the Hubble Space

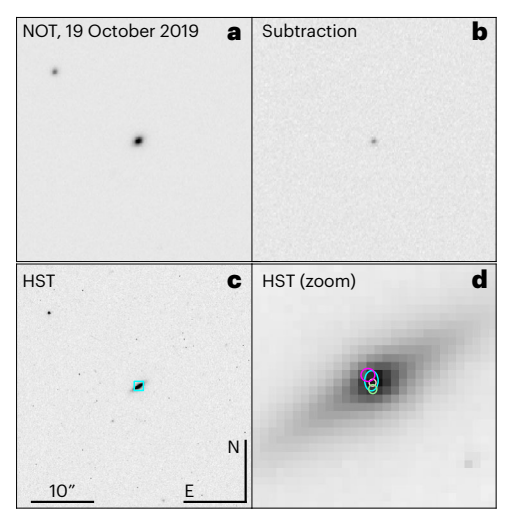


Fig. 2 | **Optical images of the afterglow of GRB 191019A and its host galaxy. a**, The *i*-band afterglow discovery image from the NOT. **b**, The result of a point spread function (PSF)-matched image subtraction with an image taken on 29 October 2019. A residual is clearly visible at the centre of the galaxy. **c**, The field as observed by the HST in April 2020, matched to the NOT images. **d**, A zoomed-in region around the host galaxy of GRB 191019A as seen with the HST (as indicated with the cyan box in panel **c**. The ellipses indicate the 2σ uncertainty regions for the optical afterglow on the host as inferred from the NOT g (cyan), r (green), i (yellow) and z (magenta). The location of the afterglow is consistent with the nucleus of the host galaxy with a projected offset, based on the i-band measurement, of $r_{\text{proj}} = 78 \pm 109$ pc.

Telescope (HST) at 30 and 184 days. None of these images reveal any evidence for transient emission to limits of typically g > 24, r > 23.5, z > 22 (Fig. 4).

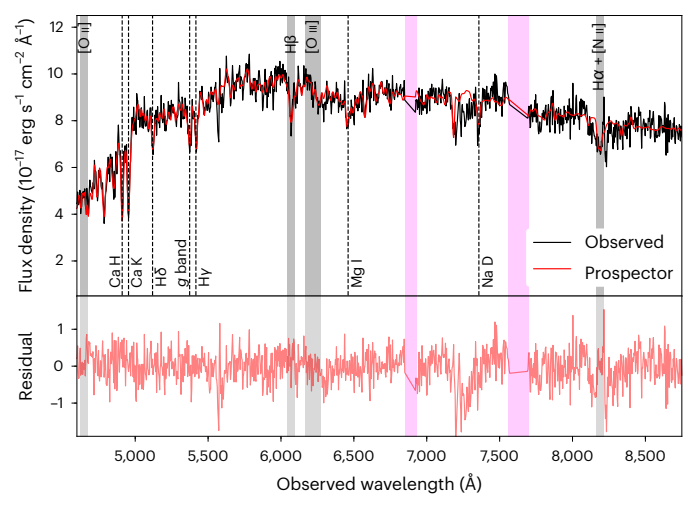


Fig. 3 | The optical spectrum of the host galaxy of GRB 191019A as observed with the NOT. The spectrum shows no emission lines associated with star formation (the expected locations of strong emission lines are marked with grey bands and telluric absorption is in pink). There is weak evidence for emission from [N II] (6,584 Å). The locations of prominent absorption features from which the redshift is determined are marked with dashed lines. Also shown are the results of a Prospector fit to the stellar spectrum (for example, omitting any emission lines). Any lines would appear in the residuals.

The non-detection of optical light between 2 and 70 days places stringent limits on any associated supernova to levels ~20 times fainter than SN 1998bw (Fig. 4; see also Methods). In fact, the deepest r-band (or F606W) limits reach absolute magnitudes of $M \approx -16$. This is comparable to the faint end of the core-collapse supernova distribution and fainter than any known stripped-envelope event found in the large sample from the Zwicky Transient Factory²¹. It is also fainter than optically selected tidal disruption events (TDEs)^{22,23}. The limiting luminosity is comparable with the peak luminosity of kilonovae. However, our observations probe much longer timescales than those of kilonovae, such that we could not rule out events similar to AT2017gfo^{24,25}. The lack of a supernova detection cannot readily be ascribed to dust extinction since the spectral energy distribution of the afterglow constrains this to be small (V-band extinction of $A_{\nu} = 0.06 \pm 0.05$; Methods). This makes GRB 191019A a member of sub-class of long GRBs without associated supernova emission. Of the GRBs at z < 0.3 with optical afterglows where supernova emission should be readily visible, and heavy extinction cannot render supernova emission undetectable, there are a total of four of these events (including GRB 191019A). In two of these (GRB 060614 and GRB 211211A), a kilonova has been observed 14-16,26,27, while GRB 060505 has also been suggested to arise from a compact object merger. The most economical hypothesis for the origin of GRB 191019A is that it belongs to the same population and is created from a compact object merger.

Combining HST ultraviolet (UV) observations with our spectroscopy and archival imaging, we fit the available photometric and spectroscopic data with the stellar population inference code Prospector (Fig. 3 and Methods). The results favour an old stellar population for the host, with the majority of stellar mass forming greater than 1 Gyr ago and little ongoing star formation $(0.06 \pm 0.03 M_{\odot} \, \text{yr}^{-1})$. The stellar mass itself is found to be $\approx 3 \times 10^{10} M_{\odot}$.

Astrometry with our early NOT observations places the location of GRB 191019A within ~100 pc of the host galaxy nucleus. This location could indicate an origin associated with the supermassive black hole which resides there, with scaling relations implying a black hole with a mass of a few $\times 10^7 M_{\odot}$ (ref. 28). However, the timescales for the emission are too short for either variability in an active galactic nucleus (AGN)

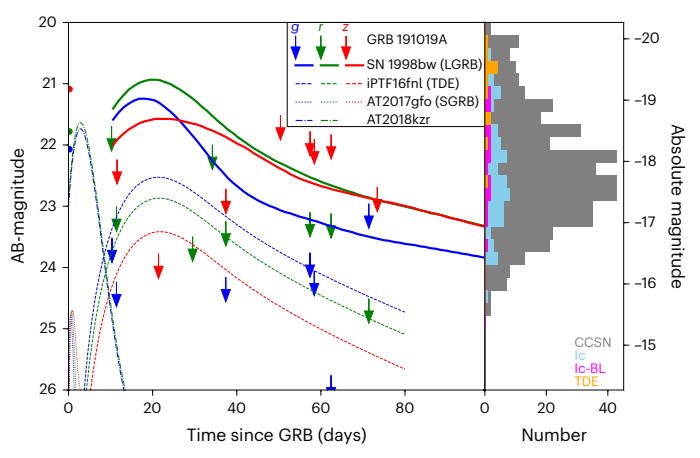


Fig. 4 | Comparison between the upper limits obtained from our targeted observations of GRB 191019A and the expectations of the light curve from supernovae or TDEs. The upper limits represent the depth of our NOT, Gemini and HST observations, while the solid lines correspond to the expectations of SN1998bw (associated with the long GRB (LGRB) 980425) at z = 0.248, based on the light curves of ref. 96. The right-hand panel shows histograms of the peak absolute magnitude distributions of core collapse supernovae (CCSN), including hydrogen-poor (Ic) and broad lined (Ic-BL) subsets and tidal disruption events (TDEs) found by the Zwicky Transient Factory (ZTF) 21,23 . Also shown are the faintest and fastest evolving TDE iPTF16fn[22,73 , AT2018kzr, which is suggested to form via a black hole—white dwarf merger 41 , and AT2017gfo, associated with GW170817 (ref. 25). Our optical observations reach a depth where we would have expected to observe the vast majority of supernovae or TDEs. However, we do not have sensitivity to detect kilonovae such as AT2017gfo. SGRB, short GRB.

or a TDE (Supplementary Information). Instead, the burst most likely arises from a stellar progenitor. The lack of a supernova and the location in an old population rule out a massive star. Instead, it appears that GRB 191019A belongs to the population of apparently long GRBs formed from compact object mergers $^{14-16}$. Its energy release and afterglow luminosity are consistent with this group of GRBs (Supplementary Information).

However, the nuclear location of the GRB on its host galaxy differs from compact object merger expectations. Systems formed via standard stellar evolution channels involve two supernovae; at each supernova, the combination of natal kicks and those induced from mass loss frequently gives the binary a substantial (50–500 km s⁻¹) systemic velocity. Furthermore, compact binary systems typically have long lifetimes before merger, which allows them to move far from their birth sites. Indeed, no short GRB with sub-arcsecond localization is consistent with the nucleus of its host galaxy²⁹.

A dynamical origin for GRB 191019A

We suggest that the binary which created GRB 191019A formed via dynamical interactions in the dense nucleus of its host galaxy. Dynamical channels for compact object formation may be due to many-body interactions in dense stellar systems such as globular clusters^{1,30} or nuclear star clusters in galaxies^{3,31}. Alternatively, they may also form at a markedly enhanced rate in the gaseous discs that surround supermassive black holes^{4,32}.

The host galaxy of GRB 191019A appears similar to those that preferentially host TDEs, with a very compact core and Balmer absorption lines. The Lick indices for H δ in absorption and H α in emission are $1.54^{+1.44}_{-0.74}$ and $2.51^{+1.81}_{-2.51}$ respectively, and are consistent with those of the TDE population which makes up only -2% of Sloan Digital Sky Survey galaxies but 75% of the TDE hosts 33 . The TDE rate effectively measures the stellar interaction rate close to the black hole. Scattering events are responsible for placing stars on paths that cross closer than the tidal radius for the star around the supermassive black hole.

The preference for TDEs in galaxies of certain types is related directly to their dense stellar environments and interaction rates³⁴. So, at face value, the host galaxy of GRB 191019A may have a dynamical interaction rate one to two orders of magnitude larger than typical galaxies.

Considering these effects and the (uncertain) intrinsic ratios of dynamical to field binaries35, we estimate that the number of dynamical mergers is typically two orders of magnitude higher than the field merger rate in locations such as that of GRB 191019A (see the detailed explanation within the Supplementary Information). This implies that it is most likely that GRB 191019A was created dynamically. However, there are considerable uncertainties, and reasonable assumptions could yield much lower ratios, although they would typically still suggest that a dynamical channel is the most likely. If GRB 191019A results from a dynamically formed compact object merger, then it may arise from several possible merger products, including neutron star-neutron star, neutron star-black hole, neutron star-white dwarf and black hole-white dwarf. The nature of the merger product and its location (for example, stellar cluster versus gas disc) should have a direct impact on the observed properties of the burst, particularly concerning duration, spectral hardness and energetics.

In the case of neutron star-neutron star or neutron star-black hole systems, one may wonder why no apparent short (<2 s) spike is observed in the prompt light curve, as in short GRBs with extended emission. The detection of the kilonova in GRB 211211A demonstrates that such a short spike is not necessarily required, although GRB 211211A appears to show other similarities to extended emission bursts³⁶. However, GRB 191019A may arise from a similar population where the contrast between 'spike' and 'extended' emission is smaller³⁷, or the extended emission is beamed with a larger opening angle than the initial spike and is unseen in this case^{38,39}. Alternatively, mergers involving white dwarfs have longer timescales naturally 40, and such an event is also possible here. Indeed, interactions in dense clusters tend to leave the more massive components in binaries, so black hole-neutron star or black hole-white dwarf mergers may be favoured³⁰. White dwarf-containing systems should yield rapid, relatively faint transients, with one event, AT2018kzr^{41,42}, suggested to arise from the merger of a white dwarf with a black hole. Our observations are not sufficiently sensitive to constrain the presence of such a signal in GRB 191019A.

Alternatively, the nuclear location also allows compact object mergers within a disc around the supermassive black hole, although there is no strong evidence for AGN activity in the host (Methods). In these discs, the compact object binaries are frequently formed by 'gas capture' mergers, which can substantially enhance the rate, despite the relatively small number of stars within the disc³². In this scenario. the long duration may well be expected, even for an intrinsically short engine. The higher densities within the disc cause the external shock to form and slow much closer to the progenitor than in bursts with a normal interstellar medium density. This extra baryon loading may effectively choke the jet^{43,44} for very high densities. However, the effect of this interaction effect smears out the prompt emission over an extended period. A very recent and explicit prediction of compact object mergers within discs is that intrinsically short-hard GRBs should become longer and softer⁴⁵, with a notable hard-soft evolution. This is exactly what is seen in GRB 191019A.

It is relevant to consider whether similar events exist within the GRB population but have been hitherto unrecognized. The vast majority of long-GRB hosts are star-forming galaxies and, where searches are possible, usually show the signatures of broad-lined type Ic supernovae. There is a small population of long bursts with deep limits on any supernova signatures ^{46,47}. Some of these have already been classified as short GRBs with extended emission ⁴⁸; however, there are additional bursts which bear further scrutiny. GRB 111005A ⁴⁹ was localized only via its radio afterglow but has deep limits on associated supernova emission. It lies in a local galaxy at only 55 Mpc and is also close to the nucleus. It could well have arisen from a compact object merger as suggested by

ref. 50 and its location raises the prospect of dynamical formation. GRB 050219A does not have a sub-arcsecond localization, but is likely to be associated with a post-starburst galaxy whose properties are similar to the host of GRB 191019A⁵¹. Finally, there are several long GRBs whose locations are consistent with their host nucleus⁵², although most of these are in star-forming hosts and are likely to have arisen from massive star collapse. Overall, the observational evidence suggests that, at most, a few per cent of the observed (long and short) GRB population forms via dynamical channels and that most of the observed systems arise via stellar (binary) evolution.

Identifying a likely dynamically produced GRB offers some of the first evidence for forming stellar-mass compact objects via dynamical channels in galactic nuclei. The mergers of such systems have received significant attention as a possible explanation for a fraction of the observed gravitational-wave population, particularly with regard to more massive black holes which can be formed via successive mergers⁵³. The gamma-ray bright population of mergers may be dwarfed by those that do not emit such high-energy flashes. In particular, very high densities within gaseous discs can result in the choking of any GRB-like emission⁴³, and black hole—black hole mergers are generally expected to be electromagnetically dark. GRBs in dense galactic nuclei therefore offer a unique new route for probing exotic compact object formation channels.

Methods

Swift observations

Burst Alert Telescope. Burst Alert Telescope (BAT) data were downloaded from the UK Swift Science Data Centre (UKSSDC^{54,55}). Reduction was performed via batgrbproduct v.2.48 from the High Energy Astrophysics software package (HEAsoft v.6.28 (ref. 56)). We extract count-rate light curves in four energy bands, 15–25 keV, 25–50 keV, 50–100 keV and 100–150 keV, using the batbinevt routine with 64 ms time bins. Spectral lag in the T_{90} interval is calculated with the Python routine signal.correlate from the scipy package⁵⁷. The time-lag is taken to be the value corresponding to the peak of the correlation coefficient and the confidence interval is $2/\sqrt{n-d}$, where n is the size of the data array and d is the measured lag⁵⁸.

To obtain the hardness ratios presented in Fig. 1, BAT spectra in the energy range 15–150 keV were extracted with batbinevt. Spectra were produced for the duration of the initial pulse complex (Fig. 1), and from the end of the initial pulse complex to T_{90} (marked 'EE' in Fig. 1), following the definitions of these epochs in refs. 37,48,59 for GRBs 080503, 060614 and 050724, respectively. Spectra were then fit in xspec v.12.11.1 with an absorbed power-law model of the form cflux*tbabs*ztbabs*pow⁶⁰, where cflux is used to measure the time-averaged flux in the 25–50 keV and 50–100 keV bands in each spectrum. Absorption in the Milky Way is fixed to the values derived in ref. 61, while flux, photon index and redshifted absorption are free parameters.

XRT. XRT data for light curves and spectral parameters are taken directly from the UKSSDC^{54,55}.

UVOT. The Swift/UVOT began observations of the field of GRB 191019A 3,294 s after the Swift/BAT trigger. The source counts used a region of 5 arcsec radius, shrinking to 3 arcsec when the count rate drops below 0.5 cps. These count rates were then corrected to 5 arcsec using the tabulated curve of growth. Background counts were extracted using three circular regions of radius 15 arcsec located in source-free regions. The count rates were obtained using the Swift tools uvotevtlc and uvot-source, respectively. At late times, the light curves are contaminated by the underlying host galaxy. To estimate the contamination, for each filter, we combined the late-time exposures (beyond 10⁷ s) until the end of observations. We extracted the count rate in the late combined exposures using the same 3 arcsec and 5 arcsec radii apertures, aperture

correcting where appropriate. These were subtracted from the source count rates. The count rates were converted to magnitudes using the UVOT photometric zero points 62,63 . To improve the signal-to-noise ratio, the count rates in each filter were binned using $\Delta t/t = 0.2$.

NOT

We obtained multiple epochs of observation of GRB 191019A with the NOT and the Alhambra Faint Object Spectrograph and Camera (ALFOSC) imaging spectrograph. Our first night's observations were obtained in the *g, r, i* and *z* bands, beginning 0.19 days after the burst. Images were reduced using standard procedures. To search for transient emission we undertook PSF-matched image subtraction⁶⁴. This revealed a clear transient source in the first epoch in all four bands. Further observations were obtained at 2.4, 3.2, 10.2, 34 and 245 days. However, these observations did not reveal any transient emission. A full log of imaging observations is shown in Supplementary Table 1.

In addition to imaging observations, we also obtained a spectrum of GRB 191019A on 19 October 2019, approximately 6 hours after the GRB. The spectrum was processed through IRAF for flat-fielding, wavelength and flux calibration.

Gemini South

We obtained observations of GRB 191019A from the Gemini South Observatory using the Gemini Multi-Object Spectrograph (GMOS). Imaging observations were obtained in the g, r and z bands at eight epochs between 11 and 70 days after the burst, with the primary aim of detecting and characterizing any associated supernova. Data were bias subtracted, flat-field corrected and combined via the Gemini IRAF package. To determine any transient contribution, we use two different approaches. The first is image subtractions which we attempted via the HOTPANTS code. These images reveal no evidence of transient emission. However, because of the compact nature of the host galaxy core, not all epochs yielded clean subtractions. Therefore, to determine limits across all epochs, we utilized the more straightforward approach of direct photometry in large (3 arcsec) apertures. There is no evidence for any variation in the galaxy with the root mean square between the different epochs corresponding to 1.3% in g, 1.0% in r and 1.5% in z. This suggests no variation in the source across the 11–70-day period of observations. To obtain limits for individual epochs, we set the host galaxy value as the mean of all epochs and subtract this from each epoch to obtain measured fluxes at each observation. These values are tabulated in Supplementary Table 1 and are plotted as 3σ upper limits in Fig. 4. Photometric calibration is performed against stars in the Panoramic Survey Telescope and Rapid Response System (Pan-STARRS) survey.

HST observations

We observed GRB 191019A with the HST at two epochs on 19 November 2019 and 24 April 2020. At each epoch, we obtained imaging observations in the F606W (exposure times of 180 s and 680 s, respectively) filter and grismspectroscopy with G800L. We reduced the imaging with the Astrodrizzle software, and subtracted the first epoch from the second. Such an analysis is complicated because in the first epoch the first image was short (180 s). Subsequently, multiple cosmic rays are present that cannot be removed by the addition of multiple images. This complicates direct photometry of the galaxy. However, subtraction of the two epochs of imaging reveals no evidence of any transient emission at the burst location. Inserting artificial stars suggests that these would be readily visible should they be brighter than F606W > 23.5 AB.

In addition to these observations, we also obtained UV observations in F225W and F275W with exposure times of 2,200 s. The data were reduced via Astrodrizzle and aligned to our NOT and Gemini observations. The host galaxy is well detected in both filters and appears extended. The resulting photometry is shown in Supplementary Table 3.

Astrometry

We performed astrometry between the images taken with the NOT on 19 October 2019 and that with the HST on 24 April 2020. We chose 20 compact sources in common to each image and derived a map between the two sets of pixel coordinates via the IRAF task geomap in each of the g, r, i and z bands. The resulting uncertainties arise from the astrometric fit and the uncertainty in the centroid of the afterglow in the NOT subtracted images. We estimate the centroid error to be 0.3 Advanced Camera for Surveys (ACS) pixels (appropriate for a signal to noise ratio (S/N) = 30 detection of the source with a seeing of ~1.0 arcsec). This is typically smaller than the error from the astrometric fit. The resulting positions are shown in Fig. 2. We find offsets of $\delta_{x(g)} = 0.44 \pm 0.82$, $\delta_{v(g)} = 0.03 \pm 1.21$, $\delta_{x(r)} = 0.43 \pm 0.50$, $\delta_{v(r)} = 1.48 \pm 0.54$, $\delta_{x(i)} = 0.30 \pm 0.41$, $\delta_{v(z)} = 0.27 \pm 0.41$, $\delta_{x(z)} = 0.85 \pm 0.91$ and $\delta_{v(z)} = -0.68 \pm 0.87$. We conclude that the source is consistent with the nucleus of the host galaxy at a projected offset (based on the i-band astrometry (best S/N)) of $r = 0.020 \pm 0.029$ arcsec or 78 ± 109 pc at z = 0.248.

Chance alignment

It is relevant to consider the probability of chance alignment of a given position with a galaxy. The location of GRB 191019A, so close to the nucleus of a relatively bright ($r \approx 19$) galaxy, leads to an extremely small chance probability. Formally, following⁶⁵, the probability of lying within 0.04 arcsec of such a host galaxy is -10⁻⁶. Therefore, even considering the ~1,000 long GRBs observed by Swift, the likelihood of a chance alignment of GRB 191019A with the nucleus of this galaxy is minimal.

The chance alignment above refers to the probability that the host galaxy is wrongly assigned. However, another relevant alignment is to consider whether the projected offset is consistent with the physical offset. That is, whether the burst truly is nuclear or whether it appearing only in projection with the host nucleus. No sub-arcsecond localized short GRBs lie at smaller projected offsets from their hosts than GRB 191019A 29 . Indeed, the solid angle for kicked events to have essentially radial kicks along our line of sight is minimal. At the same time, the chances of random orbits crossing within this distance of the nucleus are also low. This is also in keeping with the predicted offsets of compact object mergers in population synthesis $^{65-68}$, where less than 0.1–1% of mergers are typically within 70 pc of the host nucleus.

The situation is quite different for long GRBs and these bursts arise from such small offsets ~5% of the time^{52,69,70}. Indeed, for a progenitor which traces the stellar population of the host galaxy (no kicks), we may expect the chance alignment probability to be equal to the fraction of the total host light contained within the pixel hosting the event⁵². In the case of GRB 191019A, the central pixel has ~3% of the total light. However, the host galaxy of GRB 191019A is different from long-GRB host galaxies, which are typically blue, highly star-forming systems, unlike the red, quiescent host of GRB 191019A.

The zero extinction required for the afterglow could be indicative of a projection in front of any extinguishing material, especially as the galaxy has a relatively high inclination angle (~70 degrees). However, the SED fit to the galaxy suggests relatively little dust $A_v = 0.19 \pm 0.08$ globally. In quiescent galaxies such as the host of GRB 191019A, there is on average much less dust and extinction than in star-forming systems by factors of ~50 at the same stellar mass⁷¹. Indeed, the hosts of TDEs (which, as noted, are very similar to the host of GRB 191019A) do not show significant extinction. Several of these events are edge-on and robustly have low extinction (for example, ASASSN-14ae with $A_V = 0.15 \pm 0.15$ (ref. 72) and iPTF16fnl with colour excess, E(B-V) < 0.05 (ref. 73)). The demographics of these TDE hosts show an almost uniform distribution in inclination angle 74. Although there is a geometric preference for edge-on systems (that is, more systems are viewed edge-on than face-on), this suggests that the extinction effects are generally modest.

Afterglow properties

Light curve. The X-ray light curve parameters, obtained from the UKSSDC, show that the X-ray afterglow can be modelled by a single power-law with index $\alpha_1 = 1.27^{+0.17}_{-0.15}$. Alternatively, a broken power-law with $\alpha_1 = -0.14^{+0.54}_{-0.16}$, $\alpha_2 = 1.6^{+0.5}_{-0.4}$ and a break time of $t_b = (5.9^{+4.2}_{-1.8}) \times 10^3$ s also provides a good fit, although not statistically required (chance improvement probability of 4.5% or -2σ).

To place the X-ray (and early gamma-ray data) in context with the overall Swift population, we retrieve from the Swift Burst Analyser the gamma-ray and X-ray light curves of all Swift GRBs detected up until 9 October 2022. We select all GRBs with at least two detections by BAT and XRT each and a measured redshift with an accuracy of less than or equal to 0.1. In total, our sample consists of 356 long and 39 short GRBs. We processed their light curve data and moved them to their rest-frames following ref. 76. Supplementary Fig.1 shows the parameter space occupied by the long (left) and short (right) GRBs as a density plot and the BAT + XRT light curve of 191019A in blue. In both plots, we also display the light curves of GRB 050219A and 211211A (in red) and, in the right-hand panel, also highlight the short GRBs with extended emission 77.

The X-ray light curve of GRB 191019A is poorly sampled, but its evolution in luminosity space is consistent with the population of short GRBs with extended emission (Supplementary Fig. 1), while being far less consistent with the long-GRB population. This offers further support of the interpretation of GRB 191019A as belonging to the population of GRBs created via compact object mergers.

Spectral energy distribution and extinction. A straightforward way to explain the non-detection of any supernova emission would be to invoke dust extinction. To explain the non-detection of the supernova in our observations would require $A_V > 3$ mag. However, the afterglow in this case would also be subject to extinction and would be red. The detection in the UVW2 UV filter offers a strong indication that the extinction is low.

To quantify limits on the extinction, we fit the resulting X-ray–UV–optical spectral energy distribution (SED) with an obscured power-law model following the method of ref. 78. This allows either a single power-law or a cooling break between the X-ray and UV-optical regime and considers the impact of obscuration in both the soft X-ray and UV-optical regimes. This joint fit shows a single power-law slope between the X-ray and the optical and provides a measurement of $A_V = 0.06 \pm 0.05$, which confirms low extinction.

Host galaxy properties

The host galaxy is morphologically smooth and centrally concentrated (Supplementary Fig. 4). We determine the surface brightness profile via fitting elliptical isophotes to the late-time HST observations. The peak surface brightness is ~16.5 mag arcsec⁻², which is almost a magnitude brighter than, for example, the central surface brightness of the very luminous host of the short GRB 050509B (at z = 0.22, which is a similar redshift). The surface brightness profile constitutes a near-point-like source with lower surface brightness extended emission. Its 20%, 50% and 80% light radii are 0.09 arcsec, 0.27 arcsec and 0.75 arcsec. Notably, its concentration index r_{20}/r_{80} is extreme compared with most samples of galaxies⁷⁹, but comparable to those of TDE hosts (Supplementary Fig. 5). Some of this light could arise from an AGN. However, we cannot confirm this without any AGN-like emission lines in the optical spectrum of the source. A weak [N II] line is apparent in both the NOT and Gemini spectra. The absence of oxygen or hydrogen emission lines may favour a more AGN-like set of line ratios, but such an interpretation is inconclusive. A late-time observation with the Swift XRT suggests an upper limit on the 0.3–10 keV X-ray flux (F_X) of $F_x < 3 \times 10^{-14} \,\mathrm{erg} \,\mathrm{s}^{-1} \,\mathrm{cm}^{-2}$ or a luminosity of $L_x < 6 \times 10^{42} \,\mathrm{erg} \,\mathrm{s}^{-1}$. This rules out X-ray luminous AGNs, but not fainter examples. Finally, the colours in the Wide-field Infrared Survey Explorer (WISE) catalogue of W1 – W2 = 0.25 ± 0.12 lie far from the expected colours of AGNs in these bands (W1 – W2 > 0.8).

We fit the optical NOT/Alhambra Faint Object Spectrograph and Camera spectrum and broader-band photometry of the host galaxy with Prospector^{80,81}, which is a stellar population modelling inference code. Prospector samples each property parameter space with a nested sampling fitting routine, dynesty⁸², and produces model spectral energy distributions with FSPS and Python-fsps^{83,84}. We apply a Milky Way extinction law⁸⁵, Chabrier IMF⁸⁶ and a non-parametric star formation history (SFH) to the fit. We choose a non-parametric SFH model to more accurately determine when the majority of stars formed in the history of the galaxy, and thus when the progenitor was likely to have been formed. However, we note that most stellar population modelling to date uses a parametric SFH that tends to result in lower stellar masses and stellar population ages. We use a non-parametric SFH with seven age bins; the first two are between 0 Myr and 30 Myr and between 30 Myr and 100 Myr, and the final five are log-spaced from 100 Myr to the age of the universe at GRB 191019A's redshift (z = 0.248, $t_{\text{univ}} \approx 10.78 \,\text{Gyr}$). We further apply a mass-metallicity relation⁸⁷, to sample realistic masses and stellar metallicities, and a dust 2:1 ratio between the old and young stellar populations⁸⁸⁻⁹⁰. We fit the model spectral continuum with a tenth-order Chebyshev polynomial and include a nebular emission model with gas-phase metallicity and a gas-ionization parameter in the fit to measure spectral line strengths. Since the host may also contain an AGN, we also add two AGN components, which dictate the mid-IR optical depth and the fraction of AGN luminosity in the galaxy.

We find that the host of GRB 191019A has a stellar population age of $4.34^{+0.88}_{-0.47}$ Gyr (median and 1σ), stellar mass with $\log(M/M_{\odot}) = 10.57^{+0.02}_{-0.01}$ and current-day star formation rate (SFR) of $0.06^{+0.08}_{-0.03}$ M_{\odot} yr⁻¹, and thus is currently a quiescent galaxy, given the specific star formation rate (sSFR) and redshift. From a limit of the H α flux, we determine an H α SFR $< 0.12^{+0.07}_{-0.06}$ M_{\odot} yr⁻¹. We report the SFH and mass formation history of the host in terms of the lookback time ($t_{\rm lookback}$), and show the subsequent histories in Supplementary Fig. 3. We find that the majority of stellar mass and stars formed at $t_{\rm lookback}$ \gtrsim 1 Gyr, with a steep decline in mass and star formation to the present-day, and that -99% of the stellar mass was assembled greater than 1 Gyr before the merger (Supplementary Fig. 3, right). Thus, the progenitor of GRB 191019A has a higher a priori probability of forming greater than 1 Gyr ago, making it unlikely to originate from a young stellar progenitor.

As an independent check of the absence of emission lines in the host galaxy of GRB 191019A, we also fit the NOT spectrum with penalized pixel fitting pPXF 91 , where we fit only the stellar component and no emission lines following ref. 92. As with our Prospector fitting, the resulting residuals provide no evidence for emission features.

Comparison with short- and long-GRB host galaxies. We compare the stellar mass and star formation of long ⁹³ and short ⁹⁴ host galaxies with those of GRB 191019A (Supplementary Fig. 6). The long GRBs overwhelmingly favour actively star-forming hosts, with high specific SFRs. In contrast, the short GRBs span a wide range of SFRs including a fraction in quiescent systems.

There are two long-GRB host galaxies which stand out from the apparent trend. One is the host of GRB 191019A. The other is the host of GRB 050219A 51 . This burst is only localized via its X-ray afterglow, but has a comparable redshift to GRB 191019A and similar energetics (isotropic energy release ($E_{\rm iso}$) $\approx 10^{51}$ erg). With an X-ray position only, it is not possible to accurately determine whether the burst is nuclear. However, it also lies in a galaxy showing Balmer absorption lines but little evidence for star formation. Rossi et al. S1 also classify it as a post-starburst system. The similarities with GRB 191019A are striking, and we consider it to be a possible example of a similar event.

Data availability

The majority of data generated or analysed during this study are included in this published article (and its supplementary information files). Gamma-ray and X-ray data from Swift may be downloaded from the UK Swift Science Data Centre at https://www.swift.ac.uk/. HST data are associated with programmes 16051 and 16458 and can be downloaded from https://archive.stsci.edu. Gemini data are associated with programmes GS-2019B-DD-106 and GS-2019B-FT-209 and can be retrieved from https://archive.gemini.edu. NOT data can be obtained via https://www.not.iac.es/observing/forms/fitsarchive/.

Code availability

The Prospector stellar population modelling code is available at https://github.com/bd-j/prospector. The IRAF and Python scripts necessary for HST data reduction can be obtained via astroconda and IRAF (including the relevant Gemini IRAF packages) from http://www.gemini.edu/observing/phase-iii/understanding-and-processing-data/data-processing-software/gemini-iraf-general.

References

- Grindlay, J., Portegies Zwart, S. & McMillan, S. Short gamma-ray bursts from binary neutron star mergers in globular clusters. *Nat. Phys.* 2, 116–119 (2006).
- O'Leary, R. M., Meiron, Y. & Kocsis, B. Dynamical formation signatures of black hole binaries in the first detected mergers by LIGO. Astrophys. J. Lett. 824, L12 (2016).
- Fragione, G., Grishin, E., Leigh, N. W. C., Perets, H. B. & Perna, R. Black hole and neutron star mergers in galactic nuclei. *Mon. Not. R. Astron. Soc.* 488, 47–63 (2019).
- McKernan, B., Ford, K. E. S. & O'Shaughnessy, R. Black hole, neutron star, and white dwarf merger rates in AGN discs. *Mon. Not. R. Astron. Soc.* 498, 4088–4094 (2020).
- Abbott, B. P. et al. GW170817: observation of gravitational waves from a binary neutron star inspiral. *Phys. Rev. Lett.* 119, 161101 (2017).
- Arcavi, I. et al. Optical emission from a kilonova following a gravitational-wave-detected neutron-star merger. Nature 551, 64–66 (2017).
- Chornock, R. et al. The electromagnetic counterpart of the binary neutron star merger LIGO/Virgo GW170817. IV. Detection of near-infrared signatures of r-process nucleosynthesis with Gemini-South. Astrophys. J. Lett. 848, L19 (2017).
- Pian, E. et al. Spectroscopic identification of r-process nucleosynthesis in a double neutron-star merger. *Nature* 551, 67-70 (2017).
- 9. Smartt, S. J. et al. A kilonova as the electromagnetic counterpart to a gravitational-wave source. *Nature* **551**, 75–79 (2017).
- Tanvir, N. R. et al. The emergence of a lanthanide-rich kilonova following the merger of two neutron stars. Astrophys. J. Lett. 848, L27 (2017).
- Galama, T. J. et al. An unusual supernova in the error box of the y-ray burst of 25 April 1998. Nature 395, 670–672 (1998).
- Hjorth, J. et al. A very energetic supernova associated with the γ-ray burst of 29 March 2003. Nature 423, 847–850 (2003).
- Levan, A. et al. Gamma-ray burst progenitors. Space Sci. Rev. 202, 33–78 (2016).
- Rastinejad, J. C. et al. A kilonova following a long-duration gamma-ray burst at 350 Mpc. Nature 612, 223–227 (2022).
- 15. Troja, E. et al. A nearby long gamma-ray burst from a merger of compact objects. *Nature* **612**, 228–231 (2022).
- Yang, J. et al. A long-duration gamma-ray burst with a peculiar origin. Nature 612, 232–235 (2022).
- Simpson, K. K. et al. GRB 191019A: Swift detection of a burst. GRB Coord. Netw. 26031, 1 (2019).

- Krimm, H. A. et al. GRB 191019A: Swift-BAT refined analysis. GRB Coord. Netw. 26046, 1 (2019).
- Evans, P. A. et al. GRB 191019A: Swift-XRT observations. GRB Coord. Netw. 26034, 1 (2019).
- Perley, D. A. et al. GRB 191019A: NOT optical afterglow and host association confirmation. GRB Coord. Netw. 26062, 1 (2019).
- Perley, D. A. et al. The Zwicky Transient Facility Bright Transient Survey. II. A public statistical sample for exploring supernova demographics. Astrophys. J. 904, 35 (2020).
- 22. Nicholl, M. et al. Systematic light-curve modelling of TDEs: statistical differences between the spectroscopic classes. *Mon. Not. R. Astron.* Soc. **515**, 5604–5616 (2022).
- Hammerstein, E. et al. The final season reimagined: 30 tidal disruption events from the ZTF-I survey. Astrophys. J. 942, 9 (2023).
- Tanvir, N. R. et al. The emergence of a lanthanide-rich kilonova following the merger of two neutron stars. Astrophys. J. Lett. 848, L27 (2017).
- Villar, V. A. et al. The combined ultraviolet, optical, and near-infrared light curves of the kilonova associated with the binary neutron star merger GW170817: unified data set, analytic models, and physical implications. Astrophys. J. Lett. 851, L21 (2017).
- 26. Jin, Z.-P. et al. The light curve of the macronova associated with the long-short burst GRB 060614. *Astrophys. J. Lett.* **811**, L22 (2015).
- 27. Yang, B. et al. A possible macronova in the late afterglow of the long-short burst GRB 060614. *Nat. Commun.* **6**, 7323 (2015).
- 28. Kormendy, J. & Ho, L. C. Coevolution (or not) of supermassive black holes and host galaxies. *Annu. Rev. Astron. Astrophys.* **51**, 511–653 (2013).
- 29. Fong, W.-f. et al. Short GRB host galaxies. I. Photometric and spectroscopic catalogs, host associations, and galactocentric offsets. *Astrophys. J.* **940**, 56 (2022).
- 30. Ye, C. S. et al. On the rate of neutron star binary mergers from globular clusters. *Astrophys. J. Lett.* **888**, L10 (2020).
- Antonini, F. & Rasio, F. A. Merging black hole binaries in galactic nuclei: implications for advanced-LIGO detections. *Astrophys. J.* 831, 187 (2016).
- Tagawa, H., Haiman, Z. & Kocsis, B. Formation and evolution of compact-object binaries in AGN disks. *Astrophys. J.* 898, 25 (2020).
- 33. French, K. D., Arcavi, I. & Zabludoff, A. The post-starburst evolution of tidal disruption event host galaxies. *Astrophys. J.* **835**, 176 (2017).
- Stone, N. C. & Metzger, B. D. Rates of stellar tidal disruption as probes of the supermassive black hole mass function. *Mon. Not. R. Astron. Soc.* 455, 859–883 (2016).
- 35. Mandel, I. & Broekgaarden, F. S. Rates of compact object coalescences. *Living Rev. Relativ.* **25**, 1 (2022).
- Gompertz, B. P. et al. The case for a minute-long merger-driven gamma-ray burst from fast-cooling synchrotron emission. *Nat. Astron.* 7, 67–79 (2023).
- Perley, D. A. et al. GRB 080503: implications of a naked short gamma-ray burst dominated by extended emission. *Astrophys. J.* 696, 1871–1885 (2009).
- 38. Bucciantini, N., Metzger, B. D., Thompson, T. A. & Quataert, E. Short gamma-ray bursts with extended emission from magnetar birth: jet formation and collimation. *Mon. Not. R. Astron.* Soc. **419**, 1537–1545 (2012).
- 39. Lu, W. & Quataert, E. Late-time accretion in neutron star mergers: implications for short gamma-ray bursts and kilonovae. *Mon. Not. R. Astron.* Soc. **522**, 5848–5861 (2023).
- 40. King, A., Olsson, E. & Davies, M. B. A new type of long gamma-ray burst. *Mon. Not. R. Astron. Soc.* **374**, L34–L36 (2007).

- 41. McBrien, O. R. et al. SN2018kzr: a rapidly declining transient from the destruction of a white dwarf. *Astrophys. J. Lett.* **885**, L23 (2019).
- Gillanders, J. H., Sim, S. A. & Smartt, S. J. AT2018kzr: the merger of an oxygen-neon white dwarf and a neutron star or black hole. *Mon. Not. R. Astron. Soc.* 497, 246–262 (2020).
- Perna, R., Lazzati, D. & Cantiello, M. Electromagnetic signatures of relativistic explosions in the disks of active galactic nuclei. Astrophys. J. Lett. 906, L7 (2021).
- Zhu, J.-P., Zhang, B., Yu, Y.-W. & Gao, H. Neutron star mergers in active galactic nucleus accretion disks: cocoon and ejecta shock breakouts. Astrophys. J. Lett. 906, L11 (2021).
- Lazzati, D., Soares, G. & Perna, R. Prompt emission of γ-ray bursts in the high-density environment of active galactic nucleus accretion disks. Astrophys. J. Lett. 938, L18 (2022).
- Fynbo, J. P. U. et al. No supernovae associated with two long-duration y-ray bursts. *Nature* 444, 1047–1049 (2006).
- Gal-Yam, A. et al. A novel explosive process is required for the y-ray burst GRB 060614. *Nature* 444, 1053–1055 (2006).
- 48. Gehrels, N. et al. A new γ-ray burst classification scheme from GRB060614. *Nature* **444**, 1044–1046 (2006).
- Michałowski, M. J. et al. The second-closest gamma-ray burst: sub-luminous GRB 111005A with no supernova in a super-solar metallicity environment. Astron. Astrophys. 616, A169 (2018).
- Leśniewska, A. et al. The interstellar medium in the environment of the supernova-less long-duration GRB 111005A. Astrophys. J. Suppl. Ser. 259, 67 (2022).
- 51. Rossi, A. et al. A quiescent galaxy at the position of the long GRB 050219A. Astron. Astrophys. **572**, A47 (2014).
- Fruchter, A. S. et al. Long γ-ray bursts and core-collapse supernovae have different environments. *Nature* 441, 463–468 (2006).
- Fragione, G., Kocsis, B., Rasio, F. A. & Silk, J. Repeated mergers, mass-gap black holes, and formation of intermediate-mass black holes in dense massive star clusters. Astrophys. J. 927, 231 (2022).
- 54. Evans, P. A. et al. An online repository of Swift/XRT light curves of y-ray bursts. *Astron. Astrophys.* **469**, 379–385 (2007).
- Evans, P. A. et al. Methods and results of an automatic analysis of a complete sample of Swift-XRT observations of GRBs. Mon. Not. R. Astron. Soc. 397, 1177–1201 (2009).
- HEAsoft: unified release of FTOOLS and XANADU (Nasa High Energy Astrophysics Science Archive Research Center (Heasarc), 2014).
- 57. Virtanen, P. et al. SciPy 1.0: fundamental algorithms for scientific computing in Python. *Nat. Methods* 17, 261–272 (2020).
- 58. Tonry, J. & Davis, M. A survey of galaxy redshifts. I. Data reduction techniques. *Astron. J.* **84**, 1511–1525 (1979).
- 59. Barthelmy, S. D. et al. An origin for short γ-ray bursts unassociated with current star formation. *Nature* **438**, 994–996 (2005).
- Wilms, J., Allen, A. & McCray, R. On the absorption of X-rays in the interstellar medium. Astrophys. J. 542, 914–924 (2000).
- 61. Willingale, R., Starling, R. L. C., Beardmore, A. P., Tanvir, N. R. & O'Brien, P. T. Calibration of X-ray absorption in our galaxy. *Mon. Not. R. Astron.* Soc. **431**, 394–404 (2013).
- Poole, T. S. et al. Photometric calibration of the Swift ultraviolet/ optical telescope. Mon. Not. R. Astron. Soc. 383, 627–645 (2007).
- Breeveld, A. A. et al. Further calibration of the Swift ultraviolet/ optical telescope. Mon. Not. R. Astron. Soc. 406, 1687–1700 (2010).
- Alard, C. & Lupton, R. H. A method for optimal image subtraction. Astrophys. J. 503, 325–331 (1998).
- Bloom, J. S., Kulkarni, S. R. & Djorgovski, S. G. The observed offset distribution of gamma-ray bursts from their host galaxies: a robust clue to the nature of the progenitors. *Astron. J.* 123, 1111–1148 (2002).

- 66. Belczynski, K. et al. A study of compact object mergers as short gamma-ray burst progenitors. *Astrophys. J.* **648**, 1110–1116 (2006).
- 67. Church, R. P., Levan, A. J., Davies, M. B. & Tanvir, N. Implications for the origin of short gamma-ray bursts from their observed positions around their host galaxies. *Mon. Not. R. Astron. Soc.* **413**, 2004–2014 (2011).
- 68. Wiggins, B. K. et al. The location and environments of neutron star mergers in an evolving universe. *Astrophys. J.* **865**, 27 (2018).
- Blanchard, P. K., Berger, E. & Fong, W.-f. The offset and host light distributions of long gamma-ray bursts: a new view from HST observations of Swift bursts. Astrophys. J. 817, 144 (2016).
- 70. Lyman, J. D. et al. Hubble Space Telescope observations of the host galaxies and environments of calcium-rich supernovae. *Mon. Not. R. Astron.* Soc. **458**, 1768–1777 (2016).
- 71. Smith, M. W. L. et al. The Herschel Reference Survey: dust in early-type galaxies and across the Hubble Sequence. *Astrophys. J.* **748**, 123 (2012).
- 72. Holoien, T. W. S. et al. ASASSN-14ae: a tidal disruption event at 200 Mpc. *Mon. Not. R. Astron. Soc.* **445**, 3263–3277 (2014).
- 73. Blagorodnova, N. et al. iPTF16fnl: a faint and fast tidal disruption event in an E+A galaxy. *Astrophys. J.* **844**, 46 (2017).
- 74. Law-Smith, J., Ramirez-Ruiz, E., Ellison, S. L. & Foley, R. J. Tidal disruption event host galaxies in the context of the local galaxy population. *Astrophys. J.* **850**, 22 (2017).
- 75. Evans, P. A. et al. Methods and results of an automatic analysis of a complete sample of Swift-XRT observations of GRBs. *Mon. Not. R. Astron.* Soc. **397**, 1177–1201 (2009).
- 76. Schulze, S. et al. GRB 120422A/SN 2012bz: bridging the gap between low- and high-luminosity gamma-ray bursts. *Astron. Astrophys.* **566**, A102 (2014).
- 77. Gompertz, B. P., Levan, A. J. & Tanvir, N. R. A search for neutron star-black hole binary mergers in the short gamma-ray burst population. *Astrophys. J.* **895**, 58 (2020).
- Zafar, T. et al. VLT/X-shooter GRBs: individual extinction curves of star-forming regions. Mon. Not. R. Astron. Soc. 479, 1542–1554 (2018).
- Conselice, C. J. The relationship between stellar light distributions of galaxies and their formation histories. Astrophys. J. Suppl. Ser. 147, 1–28 (2003).
- Leja, J., Johnson, B. D., Conroy, C., van Dokkum, P. G. & Byler, N. Deriving physical properties from broadband photometry with Prospector: description of the model and a demonstration of its accuracy using 129 galaxies in the local universe. *Astrophys. J.* 837, 170 (2017).
- 81. Johnson, B. D., Leja, J., Conroy, C. & Speagle, J. S. Stellar population inference with Prospector. *Astrophys. J. Suppl. Ser.* **254**, 22 (2021).
- 82. Speagle, J. S. dynesty: a dynamic nested sampling package for estimating Bayesian posteriors and evidences. *Mon. Not. R. Astron. Soc.* **493**, 3132–3158 (2020).
- 83. Conroy, C., Gunn, J. E. & White, M. The propagation of uncertainties in stellar population synthesis modeling. I. The relevance of uncertain aspects of stellar evolution and the initial mass function to the derived physical properties of galaxies. *Astrophys. J.* **699**, 486–506 (2009).
- 84. Conroy, C. & Gunn, J. E. The propagation of uncertainties in stellar population synthesis modeling. III. Model calibration, comparison, and evaluation. *Astrophys. J.* **712**, 833–857 (2010).
- 85. Cardelli, J. A., Clayton, G. C. & Mathis, J. S. The relationship between infrared, optical, and ultraviolet extinction. *Astrophys. J.* **345**, 245 (1989).
- Chabrier, G. Galactic stellar and substellar initial mass function. Publ. Astron. Soc. Pac. 115, 763–795 (2003).

- 87. Gallazzi, A., Charlot, S., Brinchmann, J., White, S. D. M. & Tremonti, C. A. The ages and metallicities of galaxies in the local universe. *Mon. Not. R. Astron.* Soc. **362**, 41–58 (2005).
- 88. Price, S. H. et al. Direct measurements of dust attenuation in z ~1.5 star-forming galaxies from 3D-HST: implications for dust geometry and star formation rates. *Astrophys. J.* **788**, 86 (2014).
- Leja, J. et al. An older, more quiescent universe from panchromatic SED fitting of the 3D-HST survey. Astrophys. J. 877, 140 (2019).
- 90. Calzetti, D. et al. The dust content and opacity of actively star-forming galaxies. *Astrophys. J.* **533**, 682–695 (2000).
- 91. Cappellari, M. Full spectrum fitting with photometry in ppxf: non-parametric star formation history, metallicity and the quenching boundary from 3200 LEGA-C galaxies at redshift z≈0.8. Preprint at https://doi.org/10.48550/arXiv.2208.14974 (2022).
- 92. Inkenhaag, A., Jonker, P. G., Cannizzaro, G., Mata Sánchez, D. & Saxton, R. D. Host galaxy line diagnostics for the candidate tidal disruption events XMMSL1 J111527.3+180638 and PTF09axc. *Mon. Not. R. Astron.* Soc. **507**, 6196–6204 (2021).
- 93. Perley, D. A. et al. A population of massive, luminous galaxies hosting heavily dust-obscured gamma-ray bursts: implications for the use of GRBs as tracers of cosmic star formation. *Astrophys. J.* **778**, 128 (2013).
- 94. Nugent, A. E. et al. Short GRB host galaxies. II. A legacy sample of redshifts, stellar population properties, and implications for their neutron star merger origins. *Astrophys. J.* **940**, 57 (2022).
- 95. Lien, A. et al. The third Swift Burst Alert Telescope gamma-ray burst catalog. *Astrophys. J.* **829**, 7 (2016).
- Clocchiatti, A., Suntzeff, N. B., Covarrubias, R. & Candia, P. The ultimate light curve of SN 1998bw/GRB 980425. Astron. J. 141, 163 (2011).

Acknowledgements

A.J.L., D.B.M. and N.R.T. are supported by the European Research Council (ERC) under the European Union's Horizon 2020 research and innovation programme (grant agreement no. 725246). D.B.M. also acknowledges research grant 19054 from VILLUM FONDEN. M.N. and B.P.G. are supported by ERC under the European Union's Horizon 2020 research and innovation programme (grant agreement no. 948381), M.N. acknowledges a Turing Fellowship. The Fong Group at Northwestern acknowledges support by the National Science Foundation under grant nos. AST-1814782 and AST-1909358 and CAREER grant no. AST-2047919. W.F. gratefully acknowledges support by the David and Lucile Packard Foundation. K.E.H. acknowledges support from the Carlsberg Foundation Reintegration Fellowship Grant CF21-0103. J.H. was supported by a VILLUM FONDEN Investigator grant (project number 16599). G.L. is supported by the UK Science Technology and Facilities Council grant ST/S000453/1. A.I. acknowledges the research programme Athena with project number 184.034.002, which is financed by the Dutch Research Council (NWO). K.B. was supported by STScI HST General Observer Programmes 16548 and 16051 through a grant from STScI under National Aeronautics and Space Administration (NASA) contract NAS5-26555. The Cosmic Dawn Center is funded by the Danish National Research Foundation under grant no. 140. G.F. acknowledges support from NASA Grant 80NSSC21K1722 and NSF Grant AST-2108624 at Northwestern University. I.M. acknowledges support from the Australian Research Council through the Centre of Excellence for Gravitational Wave Discovery (OzGrav), project number CE17010004, and through Future Fellowship FT190100574. This work is partly based on observations made with the Nordic Optical Telescope, under programmes 58-502 and 61-503, owned in collaboration by the University of Turku and Aarhus University, and operated jointly by Aarhus University, the University of Turku and the University of

Oslo, representing Denmark, Finland and Norway, the University of Iceland and Stockholm University at the Observatorio del Roque de los Muchachos, La Palma, Spain, of the Instituto de Astrofísica de Canarias. It is also based on observations obtained at the international Gemini Observatory (programme IDs GS-2019B-DD-106 and GS-2019B-FT-209), a programme of NOIRLab, which is managed by the Association of Universities for Research in Astronomy (AURA) under a cooperative agreement with the National Science Foundation on behalf of the Gemini Observatory partnership: the National Science Foundation (United States), National Research Council (Canada), Agencia Nacional de Investigación y Desarrollo (Chile), Ministerio de Ciencia, Tecnología e Innovación (Argentina), Ministério da Ciência, Tecnologia, Inovações e Comunicações (Brazil) and Korea Astronomy and Space Science Institute (Republic of Korea). The data were processed using the Gemini IRAF package and DRAGONS (Data Reduction for Astronomy from Gemini Observatory North and South). In addition, this study is based on observations made with the NASA/ ESA Hubble Space Telescope obtained from the Space Telescope Science Institute, which is operated by the Association of Universities for Research in Astronomy, Inc., under NASA contract NAS5-26555. These observations are associated with programme nos. 16051 and 16458. This work made use of data supplied by the UK Swift Science Data Centre at the University of Leicester. The Pan-STARRS1 Surveys (PS1) and the PS1 public science archive have been made possible through contributions by the Institute for Astronomy, the University of Hawaii, the Pan-STARRS Project Office, the Max Planck Society and its participating institutes, the Max Planck Institute for Astronomy, Heidelberg, and the Max Planck Institute for Extraterrestrial Physics, Garching, We also thank Johns Hopkins University, Durham University, the University of Edinburgh, the Queen's University Belfast, the Harvard-Smithsonian Center for Astrophysics, the Las Cumbres Observatory Global Telescope Network Incorporated, the National Central University of Taiwan, the Space Telescope Science Institute, NASA under Grant No. NNXO8AR22G issued through the Planetary Science Division of the NASA Science Mission Directorate, the National Science Foundation Grant No. AST-1238877, the University of Maryland, Eotvos Lorand University, the Los Alamos National Laboratory and the Gordon and Betty Moore Foundation. The work is partly based on observations obtained as part of the VISTA Hemisphere Survey, ESO Progam, 179.A-2010 (PI: McMahon). We made use of data products from the Wide-field Infrared Survey Explorer. which is a joint project of the University of California, Los Angeles, and the Jet Propulsion Laboratory/California Institute of Technology, funded by NASA.

Author contributions

A.J.L. obtained, reduced and analysed observations and wrote the text. D.B.M. obtained and reduced the NOT observations, performed subtractions and photometry and contributed to analysis and interpretation. B.P.G. undertook the Swift BAT and XRT analyses and contributed to analysis and interpretation. A.E.N. performed analysis of the host galaxy with Prospector. M.N. contributed to the light curve, TDE sections and spectral analysis. S.R.O. analysed the UVOT data. D.A.P. contributed to the NOT observations and interpretation. J.R. worked with the Gemini observations, photometry and subtractions. B.D.M. contributed to the theoretical discussion and interpretation. S.S. provided the comparison between the X-ray/gamma-ray light curves of GRB 191019A and other bursts. E.R.S. worked on population modelling of the host galaxy. A.I. performed the fit of the spectrum with pPXF. A.A.C. investigated the host population and contributed to interpretation. K.B. and A.F. worked on the HST observations and provided comments. A.d.U.P. worked on the NOT observations and commented on the text. W.F. worked on the interpretation. G.F. provided theoretical interpretation. J.P.U.F. led the first NOT observations and provided comments. N.G. worked on the offset

implications. K.E.H. worked on the NOT data and interpretation.
J.H. worked on interpretation and text. P.G.J. worked on the interpretation, in particular, with regard to TDE possibilities.
G.L. worked on the interpretation and I.M. provided theoretical input.
J.S. and P.J. worked on the NOT data and provided comments.
N.R.T. was involved in the NOT, Gemini and HST observations.

Competing interests

The authors declare no competing interests

Additional information

Supplementary information The online version contains supplementary material available at https://doi.org/10.1038/s41550-023-01998-8.

Correspondence and requests for materials should be addressed to Andrew J. Levan.

Peer review information *Nature Astronomy* thanks the anonymous reviewers for their contribution to the peer review of this work.

Reprints and permissions information is available at www.nature.com/reprints.

Publisher's note Springer Nature remains neutral with regard to jurisdictional claims in published maps and institutional affiliations.

Springer Nature or its licensor (e.g. a society or other partner) holds exclusive rights to this article under a publishing agreement with the author(s) or other rightsholder(s); author self-archiving of the accepted manuscript version of this article is solely governed by the terms of such publishing agreement and applicable law.

© The Author(s), under exclusive licence to Springer Nature Limited 2023

Department of Astrophysics/IMAPP, Radboud University, Nijmegen, the Netherlands. Department of Physics, University of Warwick, Coventry, UK. 3Cosmic Dawn Center (DAWN), Copenhagen, Denmark. 4Niels Bohr Institute, University of Copenhagen, Copenhagen, Denmark. 5DTU Space, Technical University of Denmark, Lyngby-Taarbæk, Denmark. 6Institute for Gravitational Wave Astronomy and School of Physics and Astronomy, University of Birmingham, Birmingham, UK. ⁷Center for Interdisciplinary Exploration and Research in Astrophysics and Department of Physics and Astronomy, Northwestern University, Evanston, IL, USA. 8 Astrophysics Research Institute, Liverpool John Moores University, Liverpool, UK. 9Center for Computational Astrophysics, Flatiron Institute, New York, NY, USA. 10Department of Physics and Columbia Astrophysics Laboratory, Columbia University, New York, NY, USA. 11 Department of Physics, The Oskar Klein Center, Stockholm University, AlbaNova, Stockholm, Sweden. ¹²SRON, Netherlands Institute for Space Research, Leiden, the Netherlands. ¹³Australian Astronomical Optics, Macquarie University, City of Ryde, New South Wales, Australia. 14Astronomy, Astrophysics and Astrophotonics Research Centre, Macquarie University, Sydney, New South Wales, Australia. 15 Instituto de Astrofísica de Andalucía (IAA-CSIC), Granada, Spain. 16 Space Telescope Science Institute, Baltimore, MD, USA. ¹⁷Université Côte D'Azur, Observatoire de la Côte D'Azur, CNRS, Artemis, Nice, France. ¹⁸DARK, Niels Bohr Institute, University of Copenhagen, Copenhagen, Denmark. 19 Centre for Astrophysics and Cosmology, Science Institute, University of Iceland, Reykjavík, Iceland. 20 School of Physics and Astronomy, University of Leicester, Leicester, UK. 21 Monash Centre for Astrophysics, School of Physics and Astronomy, Monash University, Melbourne, Victoria, Australia. ²²OzGrav, ARC Centre of Excellence for Gravitational Wave Discovery, Hawthorn, Victoria, Australia. ²³Jodrell Bank Centre for Astrophysics, Department of Physics and Astronomy, The University of Manchester, Manchester, UK. 24INAF, Astronomical Observatory of Brera, Merate (LC), Italy. ²⁵Department of Astronomy, The Oskar Klein Center, Stockholm University, AlbaNova, Stockholm, Sweden. e-mail: a.levan@astro.ru.nl